Non-coding RNA Research 9 (2024) 1098–1110

Contents lists available at ScienceDirect

Non-coding RNA Research

journal homepage: www.keaipublishing.com/en/journals/non-coding-rna-research

Original Research Article

MiR-200b-3p elevates 5-FU sensitivity in cholangiocarcinoma cells via autophagy inhibition by targeting KLF4

Feng Peng [a,1], Ruizhi He [a,1], Yuhui Liu [a], Yu Xie [a], Guangbing Xiong [a], Xu Li [a], Min Wang [a], Chunle Zhao [a,**], Hang Zhang [a,***], Simiao Xu [b,****], Renyi Qin [a,*]

[a] Department of Biliary-Pancreatic Surgery, Affiliated Tongji Hospital, Tongji Medical College, Huazhong University of Science and Technology, Wuhan, 430030, China
[b] Division of Endocrinology, Affiliated Tongji Hospital, Tongji Medical College, Huazhong University of Science and Technology, Branch of National Clinical Research Center for Metabolic Disease, Wuhan, Hubei, 430030, China

ARTICLE INFO

Keywords:
miR-200b-3p
Autophagy
KLF4
Chemosensitivity
Cholangiocarcinoma

ABSTRACT

Cholangiocarcinoma is one of the most lethal human cancers, and chemotherapy failure is a major cause of recurrence and poor prognosis. We previously demonstrated that miR-200 family members are downregulated in clinical samples of cholangiocarcinoma and inhibit cholangiocarcinoma tumorigenesis and metastasis. However, the role of differentially expressed miR-200b-3p in 5-fluorouracil chemosensitivity remains unclear. Here, we examined how miR-200b-3p modulates 5-fluorouracil chemosensitivity in cholangiocarcinoma. We observed that miR-200b-3p was associated with 5-fluorouracil sensitivity in cholangiocarcinoma and increased 5-fluorouracil-induced mitochondrial apoptosis in cholangiocarcinoma cells. Mechanistically, miR-200b-3p suppressed autophagy in cholangiocarcinoma cells to mediate 5-fluorouracil sensitivity. Further, we identified KLF4 as an essential target of miR-200b-3p in cholangiocarcinoma. Notably, the miR-200b-3p/KLF4/autophagy pathway augmented the chemosensitivity of cholangiocarcinoma cells to 5-fluorouracil. Our findings underscore the key role of miR-200b-3p in chemosensitivity to 5-fluorouracil and highlight the miR-200b-3p/KLF4/autophagy axis as a potential therapeutic target for cholangiocarcinoma.

1. Introduction

Cholangiocarcinoma (CCA) is a lethal human cancer that is considered difficult to treat, and prognosis remains poor [1]. Despite advances in early diagnosis and treatment, the 2-year overall survival rate is only 65%, which can be attributed to the biological characteristics of CCA [2]. For CCA recurrence and distant metastasis, surgical outcomes tend to be limited [3]. Thus, chemotherapy remains a significant component of treatment for CCA [4]. 5-fluorouracil (5-FU) is the most commonly used chemotherapeutic drug for CCA. Nevertheless, the dose-dependent response to 5-FU in CCA is limited, as a high dose of 5-FU produces severe side effects, whereas a low dose of 5-FU results in chemoresistance and low efficacy [5]. Therefore, elucidating the mechanisms underpinning chemoresistance in CCA remains a critical unmet need.

Autophagy is an evolutionarily conserved catabolic process that is crucial for the degradation of cellular proteins or components and maintenance of homeostasis [6]. During autophagy, impaired organelles are sequestered in double-membrane vesicles for lysosomal degradation [7]. Mitophagy is a distinct form of autophagy in which damaged mitochondria are selectively degraded to maintain cellular function and integrity [8]. Dysregulation of autophagy/mitophagy has been linked to many human diseases, including cancers [8–10]. Cancer cells have not only inherited autophagic mechanisms to survive in extreme tumor microenvironments, but have also evolved to increase invasiveness and resistance to anticancer drugs such as chemotherapy [11]. Therefore, CCA treatment may benefit from approaches that inhibit autophagy.

MicroRNAs (miRNAs) are regulatory non-coding RNAs approximately 22 nucleotides in length [12]. miRNAs are assembled into an RNA-induced silencing complex (RISC), which localizes directly to the target 3′-untranslated region (3′-UTR) of mRNAs, triggering

* Corresponding author.
** Corresponding author.
*** Corresponding author.
**** Corresponding author.
E-mail addresses: dr.zhaocl@outlook.com (C. Zhao), zhanghang@hust.edu.cn (H. Zhang), tjxusimiao@126.com (S. Xu), ryqin@tjh.tjmu.edu.cn (R. Qin).
[1] Feng Peng and Ruizhi He have contributed equally to this work.

https://doi.org/10.1016/j.ncrna.2024.06.004
Received 2 February 2024; Received in revised form 9 May 2024; Accepted 4 June 2024
Available online 7 June 2024

posttranscriptional regulation [13]. It is well established that miRNAs play a vital role in cancer progression [14]. In CCA, abnormal expression of miRNAs has been reported, and alterations in miRNAs can contribute to tumor growth by modulating critical genes involved in tumor cell survival [15]. Among the miRNAs, miR-200b-3p is thought to play a critical role in the regulation of growth and chemotherapy sensitivity of CCA cells [15,16]. A previous study demonstrated that the expression profile of miR-200b-3p was associated with 5-FU chemoresistance and self-renewal capacity in CCA cells [16]. However, the mechanism by which miR-200b-3p regulates these processes is unclear. Moreover, there has been a paucity of research on the role of miR-200b-3p in CCA to date. Here, we demonstrated that forced expression of miR-200b-3p, which inhibited autophagy by directly targeting Krüppel-like factor 4 (KLF4), enhanced the chemosensitivity of CCA cells to 5-FU. Our results provide a novel strategy for treating CCA.

2. Materials and methods

2.1. Cell lines, clinical samples and chemicals

Human CCA TFK-1 cells were purchased from DSMZ (Braunschweig, Germany). HuCCT-1 cells were kindly provided by Jianmin Wang, Affiliated Tongji Hospital. Cells were cultured in RPMI-1640 medium supplemented with 10% fetal bovine serum (FBS) at 37 °C in a 5% CO_2 incubator. Human cholangiocarcinoma tissues were obtained from patients with postoperative pathological diagnosed perihilar or distal biliary cholangiocarcinoma at the Department of Biliary-Pancreatic Surgery, Affiliated Tongji Hospital (Hubei, China). Human sample collection procedures were approved by the China Ethical Review Committee. 5-FU (F6627) and CQ (C6628) were obtained from Sigma-Aldrich (St. Louis, MO, USA). EBSS (24010043) was obtained from Thermo Fisher. Anti-LC3B (3868), anti-SQSTM1/p62 (8025), anti-PARP (9532), anti-cleaved PARP (5625), anti-BID (2002), anti-MFN2 (9482), anti-OPA1 (80471), anti-KLF4 (12173), anti-caspase-3 (9665), anti-cleaved caspase-3 (9664), anti-caspase-8 (4790), and anti-caspase-12 (35965) antibodies were obtained from Cell Signaling Technology (Beverly, MA, USA). Anti-Bax (50599-2-Ig), anti-KLF4 (11880-1-AP), and anti-GAPDH (60004-1-Ig) antibodies were obtained from Proteintech Group (Chicago, IL, USA). Anti-Ki67 (sc-15402) and anti-LAMP1 (sc-18821) antibodies were obtained from Santa Cruz Biotechnology (Santa Cruz, CA, USA).

2.2. Cell viability and colony formation assays

Cell viability was assessed using the CCK-8 assay (Dojindo Molecular Technologies, Kumamoto, Japan) according to the manufacturer's instructions. Briefly, cells were plated in a 96-well plate at a concentration of 2000 cells per well. At the indicated time points, CCK-8 (Beyotime Institute of Biotechnology) was added to each well, and the cells were incubated at 37 °C for 2 h. The plate was measured using a microplate reader (Bio-Tek Elx 800, USA) at 450 nm. The IC50 (the concentration at which the optical density was reduced by 50%) was calculated using linear regression performed on the linear zone of the dose-response curve. For the colony-forming assay, cells were seeded in 6-well plates at a concentration of 1000 cells per well. The medium was replaced with fresh medium, and the cells were allowed to grow for 14 days. The cells were fixed in 4% paraformaldehyde, stained with 0.5% cresyl violet, and imaged to quantify the colonies. All experiments were repeated at least three times.

2.3. Annexin V-FITC/PI apoptosis assay

Cell apoptosis was detected using the annexin V-FITC/PI Apoptosis Detection Kit (MultiSciences, Hangzhou, China) according to the manufacturer's instructions. In brief, cells were resuspended in 1 × binding buffer with annexin V-FITC (2.5 μL per well) and PI (5 μL per well) and incubated in the dark for 15 min at 37 °C. Cells were analyzed using flow cytometry on a FACSCalibur flow cytometer (BD Immunocytometry Systems, USA).

2.4. Measurement of mitochondrial membrane potential

Mitochondrial membrane potential (MMP, Δψm) was analyzed using the fluorescent dye JC-1, according to the manufacturer's instructions. Briefly, cells were centrifuged at 1000 rpm for 5 min at room temperature. Following incubation with JC-1 (5 μg/mL) for 20 min at 37 °C, cells were washed and analyzed by flow cytometry on a FACSCalibur flow cytometer (BD Immunocytometry Systems, USA).

2.5. Real-time PCR

Total RNA was reverse-transcribed to cDNA using a TaqMan MicroRNA Reverse Transcription Kit (Applied Biosystems, USA) or PrimeScript Reverse Transcription Kit (Takara, Japan) after extraction with TRIzol reagent (Invitrogen, USA). Quantitative real-time PCR was performed using TaqMan MicroRNA assay (Applied Biosystems) for miRNA analysis or the SYBR Green Real-Time PCR Premix (Takara, Japan) for mRNA analysis according to the manufacturer's instructions. Gene expression was measured using a CFX96 Real-Time PCR System (Bio-Rad, USA). The housekeeping genes *GAPDH* or *U6* were used as reference genes in all RT-qPCR analyses. The following primers were used: *SCD* 5′-TCTAGCTCCTATACCACCACCA-3′ (forward), 5′-TCGTCTCCAACTTATCTCCTCC-3′ (reverse); *PSAT1* 5′-TGCCGCACTCAGTGTTGTTAG-3′ (forward), 5′-GCAATTCCCGCACAAGATTCT-3' (reverse); *KRT80* 5′- CCTCCCTAATTGGCAAGGTG-3' (forward), 5′-AGATGCCCGAGGTCGAAGAT-3′ (reverse); *KLF4* 5′-CCATCTTTCTCCACGTTCG-3′ (forward), 5′-AGTCGCTTCATGTGGGAGAG-3′ (reverse); and *FSTL4* 5′-TCCTGGGAAAGAGGATCACCG-3′ (forward), 5′-TCTGCATCTAAGTCCCTGAACA-3′ (reverse).

2.6. Western blot analysis

Total cellular proteins were extracted using a RIPA buffer kit with a protease inhibitor (Boster Biological Technology, Wuhan, China). Protein concentration was measured using a bicinchoninic acid protein assay kit (Beyotime, Haimen, China). Equivalent amounts of protein from the samples were resolved on an SDS-PAGE gel, transferred onto a polyvinylidene fluoride membrane (Millipore, Burlington, MA, USA), and incubated with the indicated primary antibodies and relevant secondary antibodies. The blots were detected using a ChemiDoc XRS System (Bio-Rad Laboratories, USA).

2.7. Transmission electron microscopy

Cell samples were fixed in 2.5% glutaraldehyde in 0.1 M cacodylate buffer at 4 °C overnight and then postfixed with 1% osmium tetroxide in 0.1 M cacodylate buffer for 1 h at 4 °C. After dehydration in a graded series of ethanol, the samples were embedded in spur resin and sliced into serial sections with an ultramicrotome. Sections were stained with 4% uranyl acetate and lead citrate. Images were captured using a Hitachi H-7000FA transmission electron microscope.

2.8. Immunofluorescence and confocal microscopy

For immunofluorescence analysis, the indicated treated cells were seeded on glass coverslips. After fixed with 4% formaldehyde and permeabilized with 0.1% Triton X-100, the cells were incubated with primary antibodies overnight and Cy3 conjugated secondary antibody for 2 h at room temperature. The cells subsequently visualized under a confocal microscope (Carl Zeiss, Germany, LSM710).

For immunofluorescence analysis of LC3, cells were treated with the designated treatments after transfection with GFP-mRFP-LC3B or GFP-

LC3B. Cells were grown on glass coverslips. After adhesion, the cells were fixed with 4% formaldehyde and imaged using a confocal microscope (Carl Zeiss, Germany, LSM710).

2.9. Transfection and generation of stable cell lines

The miR-200b-3p inhibitor, its control (anti-miR Ctrl), miR-200b-3p mimic and corresponding negative control (NC) were purchased from Ribobio (Guangzhou, China). To generate the KLF4 plasmid, fragments of KLF4 were cloned into a pHAGE plasmid. To generate the shKLF4 plasmid, fragments of shRNA targets were cloned into the AgeI-EcoRI site of pLKO.1. Cells were transfected using Lipofectamine 2000 (Invitrogen, Carlsbad, CA, USA) according to the manufacturer's instructions. Lentiviruses containing miR-200b-3p, relevant controls, and tandem-labeled GFP-mRFP-LC3 reporter were constructed by GenePharma (Shanghai, China). Viral supernatant stably downregulated KLF4 was produced by co-transfection of HEK293T cells with shKLF4 plasmid, the pMD2.G envelope plasmid and the psPAX packaging plasmid. Lentivirus transfection was performed according to the manufacturer's instructions.

2.10. Luciferase reporter assay

To generate KLF4 3′-UTR wild-type plasmids, the appropriate 3′-UTR fragments were cloned into the psi-CHECK2 luciferase reporter vector (Promega, WI, USA). To generate KLF4 3′-UTR mutated luciferase reporter plasmids, mutant KLF4 3′-UTR fragments were constructed by deleting the miR-200b-3p targeting sequence in the 3′UTR region. Luciferase activity was determined using a dual-luciferase reporter assay system (Promega, Madison, WI, USA) according to the manufacturer's instructions. Relative luciferase activity was determined using a GloMax 20/20 luminometer (Promega). Luciferase activity was normalized to that of firefly luciferase.

2.11. RNA-seq

Total RNA from cell samples was sent to BGI (Beijing Genomics Institute) using the BGISEQ-500 platform for sequencing. Briefly, RNA was sheared and reverse transcribed using random primers to obtain cDNA. After adaptor ligation, the products were purified and amplified for library construction. The prepared library was sequenced, and differentially expressed genes were analyzed according to the manufacturer's protocol.

2.12. Xenograft experiments

All experimental procedures were approved by the Institutional Animal Care and Use Committee of the Huazhong University of Science and Technology. Six-week-old female BALB/c nude mice obtained from HFK BioTechnology were randomly divided into groups as indicated and subcutaneously injected with the indicated cells (2×10^6 cells per mouse), which were mixed with Matrigel (Becton Dickinson, USA) at a 1:1 ratio. Tumor-bearing mice were intraperitoneally treated with either vehicle or 5-FU (15 mg/kg). The tumor size and body weight of the mice were measured once a week from the time of implantation. Tumor volume was calculated using the following formula: volume (mm^3) = length × $width^2/2$.

2.13. Statistical analysis

All data are presented as the mean ± standard deviation (SD). Significance was evaluated using a Student's t-test. Statistical analyses were performed using GraphPad Prism 5 software and SPSS software (version 22.0; SPSS, Chicago, USA). Statistical significance was set at $p < 0.05$.

3. Results

3.1. MiR-200b-3p enhances the chemosensitivity of CCA cells to 5-FU

To evaluate the effects of miR-200b-3p on chemotherapy for CCA, cell counting kit-8 (CCK8) assays were performed to assess cell viability. We previously demonstrated that miR-200b-3p was underexpressed in CCA [16]; hence, we performed gain-of-function studies. Ectopic expression of miR-200b-3p reduced the growth of TFK-1 and HuCCT-1 cells (Fig. 1A). To investigate the association between miR-200b-3p and chemoresistance in CCA, the IC50 values of 5-FU were tested in miR-200b-3p-overexpressing and control CCA cells. We calculated the IC50 values of CCA cells using the CCK-8 assay upon exposure to step-up concentrations of 5-FU for 24 h. The IC50 value of TFK-1 NC cells was 80.79 ± 13.45 (n = 3), and the IC50 value of TFK-1 miR-200b-3p cells was 32.25 ± 3.30 (n = 3). The IC50 value of HuCCT-1 NC cells was 100.80 ± 8.37 (n = 3), and the IC50 value of HuCCT-1 miR-200b-3p cells was 52.88 ± 3.12 (n = 3). These results suggest that miR-200b-3p-overexpressing cells were sensitive to 5-FU (Fig. 1B). Further analyses of long-term cell viability confirmed that miR-200b-3p significantly decreased colony formation of TFK-1 and HuCCT-1 cells. This difference in potency was more evident in the presence of 5-FU (Fig. 1C). To confirm this finding *in vivo*, we established xenografts of subcutaneously implanted TFK-1 cells using control and miR-200b-3p overexpression lentivirus-based vectors. Tumor-bearing mice were intraperitoneally administered either vehicle or 5-FU twice per week. In the sixth week, elevated miR-200b-3p expression decreased tumor size in subcutaneous models in nude mice and augmented the suppression of tumor size in 5-FU-treated animals (Fig. 1D and E). Further, overexpression of miR-200b-3p prevented weight loss caused by tumor-bearing (Fig. 1E). miR-200b-3p overexpression combined with 5-FU treatment resulted in slight body weight loss, but no significant difference was observed relative to controls in the presence of 5-FU (Fig. 1E). Immunohistochemistry staining of paraffin-embedded samples from xenograft tumors revealed that Ki67 was lower in miR-200b-3p overexpression group versus the control group. And overexpression of miR-200b-3p led to a dramatically decrease of Ki67 staining in the presence of 5-FU treatment (Fig. 1F and G). Cleaved caspase-3 staining showed a significant increase in miR-200b-3p overexpression group compared with the control. And 5-FU treatment aggravated the difference between the two groups (Fig. 1F and H). These data suggest that miR-200b-3p plays a key role in the regulation of CCA cell growth and enhances the chemosensitivity of CCA cells to 5-FU.

3.2. MiR-200b-3p increases 5-FU-induced mitochondrial apoptosis of CCA cells

Increasing evidence suggests that inhibitory cell growth is closely associated with cell apoptosis [17]. Therefore, we hypothesized that apoptosis plays a key role in miR-200b-3p-induced chemosensitivity to 5-FU in CCA cells. we first performed annexin V/PI staining assays to determine the apoptotic ratio of CCA cells using flow cytometry. We observed that ectopic miR-200b-3p expression increased the apoptotic ratio of CCA cells compared to that in the control group (Fig. 2A). The miR-200b-3p-elicited apoptotic effect was exacerbated in the presence of 5-FU (Fig. 2A). We next performed western blotting to examine the levels of apoptosis signal-related proteins PARP, cleaved PARP, caspase-3, caspase-8 and caspase-12, which are considered markers of apoptosis [18]. In the presence of 5-FU, miR-200b-3p overexpression decreased PARP and caspase-3 expression and induced cleavage of PARP, but not caspase-8 and caspase-12 in TFK-1 and HuCCT-1 cells (Fig. 2B).

Mitochondrial dysfunction plays a critical role in cancer chemoresistance in cells [19]. To evaluate the role of mitochondrial dysfunction in miR-200b-3p-elicited 5-FU chemosensitivity in CCA cells, the mitochondrial membrane potential ($\Delta\psi m$) and expression of

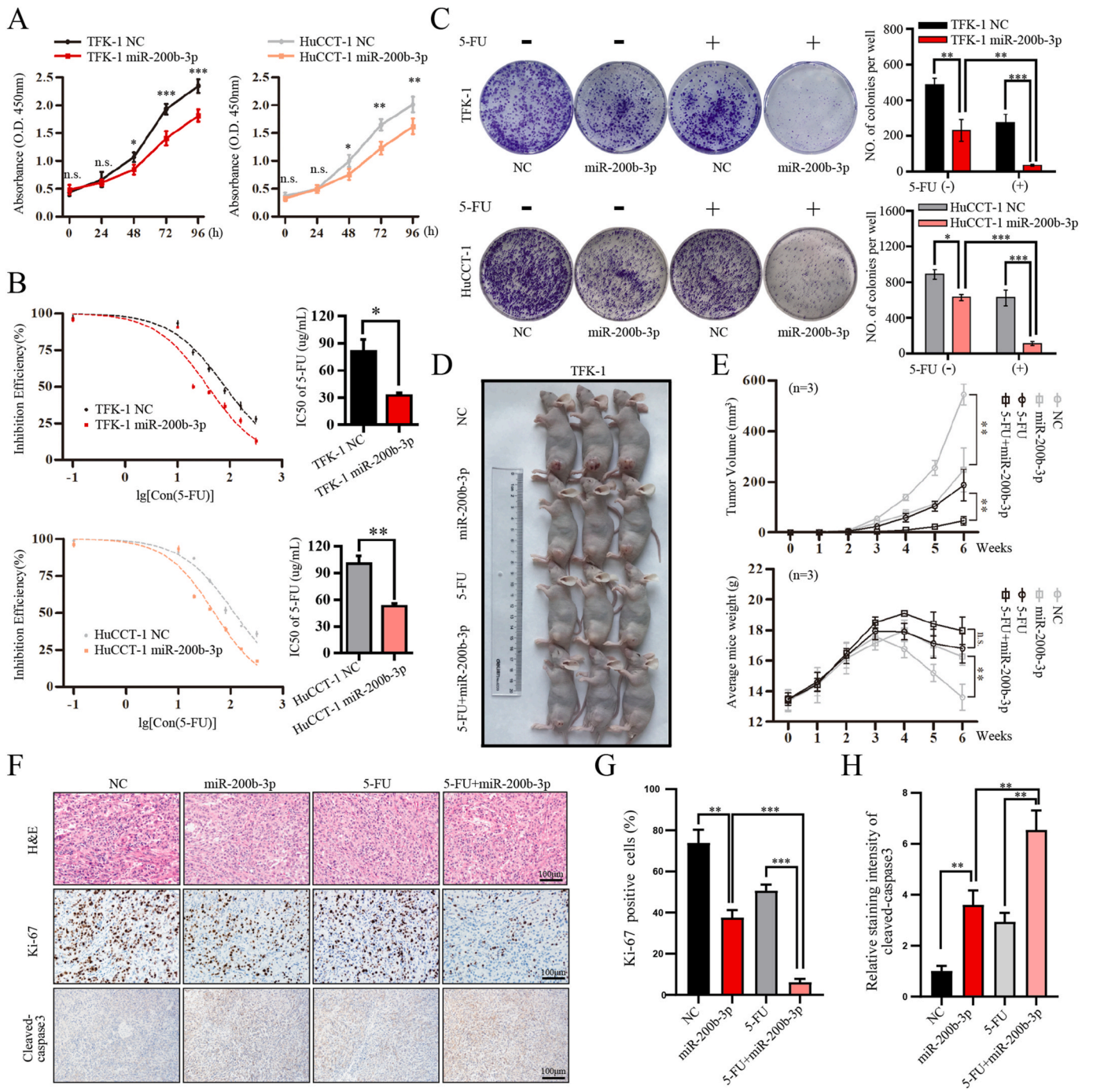

Fig. 1. MiR-200b-3p promotes 5-FU sensitivity in CCA cells. (A) Viability of TFK-1 and HuCCT-1 cells expressing NC or miR-200b-3p detected using a CCK8 assay. (B) Sensitivity of cells to 5-FU was evaluated using the CCK8 assay upon exposure to step-up concentrations of 5-FU for 24 h. Dose-effect curves and statistical analysis of IC50 values are presented in the left and right panels, respectively. *$p < 0.05$; **$p < 0.01$. (C) Representative images from the colony-forming assay and colony number analysis of TFK-1 and HuCCT-1 cells stably expressing NC or miR-200b-3p in the absence or presence of 40 μg/mL of 5-FU treatment. All experiments were performed in triplicate. Data are presented as the mean ± SD. (D) Tumors from mice in each group in week 6 after tumor implantation are presented. (E) The tumor volume (upper panel) and body weight (lower panel) of the mice in each group were measured once a week from the time of tumor implantation. (F) Representative images of immunohistochemistry staining showing H&E, Ki67 and cleaved caspase-3 in xenograft tumor tissues from the different experimental mouse groups. Scale bar, 100 μm. (G) Statistical analysis of percentage of Ki67 positive cells from xenograft tumor tissues. (H) Statistical analysis of staining intensity of cleaved caspase-3 from xenograft tumor tissues.

mitochondrial apoptosis-related proteins were assessed. We observed that Δψm was significantly decreased in miR-200b-3p-overexpressing cells compared with control group. Elevated miR-200b-3p resulted in a more severe loss of Δψm in the presence of 5-FU (Fig. 2C). Combination treatment of 5-FU and miR-200b-3p increased Bax protein levels and decreased BID protein levels, as detected using western blot (Fig. 2D). Collectively, these data indicate that mitochondrial dysfunction plays a vital role in the regulation of miR-200b-3p-induced mitochondrial apoptosis in CCA cells caused by 5-FU.

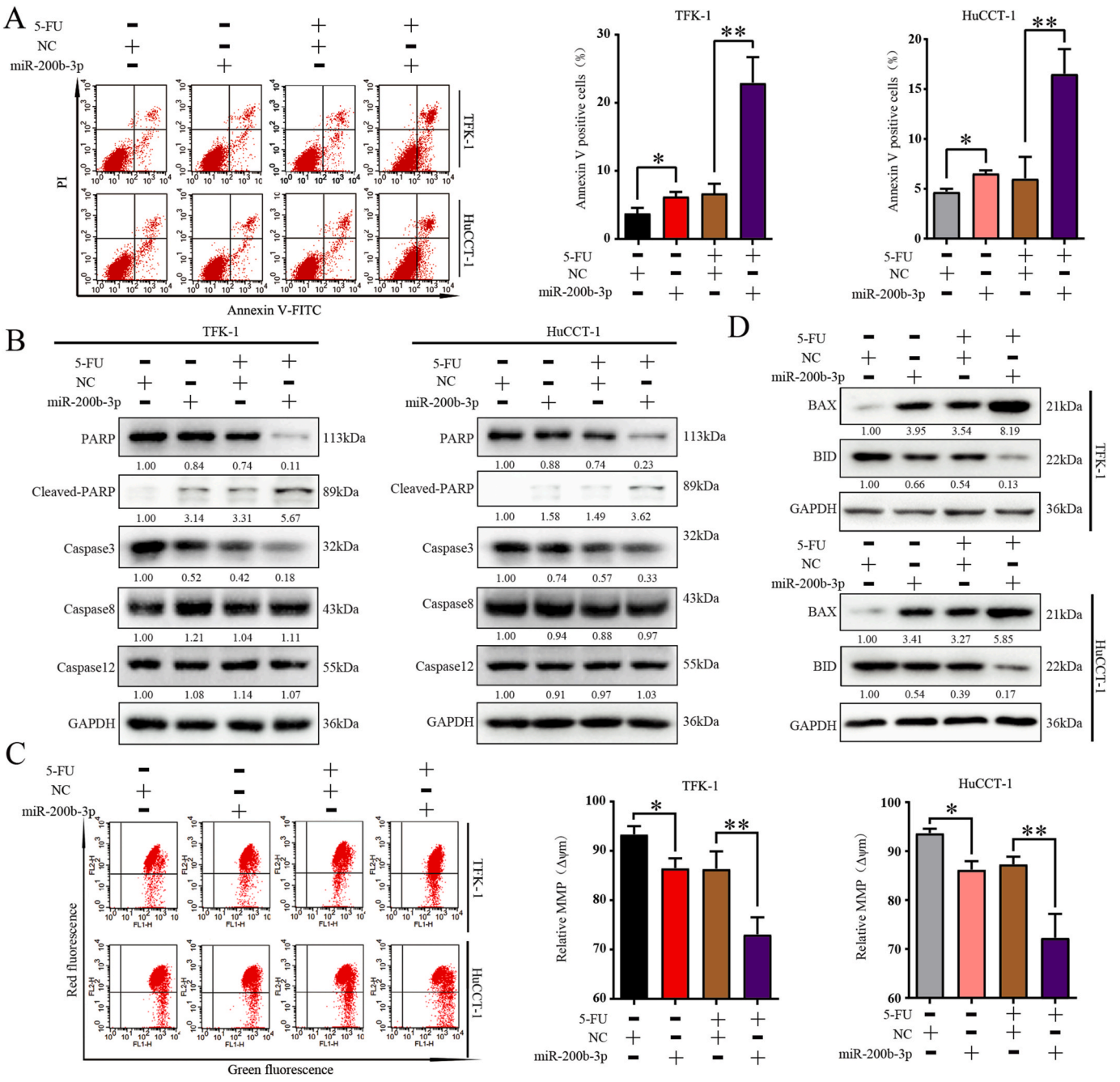

Fig. 2. MiR-200b-3p increases 5-FU-induced mitochondrial apoptosis in CCA cells. (A) Flow cytometry detecting apoptotic cells in indicated cells stably expressing NC or miR-200b-3p in the absence or presence of 40 μg/mL of 5-FU treatment. *$p < 0.05$; **$p < 0.01$. (B) Western blot analysis of PARP, cleaved PARP, caspase-3, caspase-8 and caspase-12 in TFK-1 and HuCCT-1 cells stably expressing NC or miR-200b-3p in the absence or presence of 40 μg/mL of 5-FU treatment. (C) MMP (Δψm) was detected in cells stably expressing NC or miR-200b-3p in the absence or presence of 40 μg/mL of 5-FU treatment. *$p < 0.05$; **$p < 0.01$. (D) Western blot analysis of the mitochondrial apoptosis-related proteins BID and BAX in TFK-1 and HuCCT-1 cells stably expressing NC or miR-200b-3p in the absence or presence of 40 μg/mL of 5-FU treatment.

3.3. MiR-200b-3p mediates 5-FU sensitivity by suppressing autophagy in CCA cells

The occurrence of mitochondrial apoptosis implies deficits in mitochondrial quality control mechanisms, whereby a specialized autophagy pathway (mitophagy) maintains the removal of damaged mitochondria [20]. To investigate the involvement of mitophagy in miR-200b-3p-mediated regulation of CCA cell apoptosis, we analyzed autophagic marker microtubule-associated protein 1 light chain 3β (LC3B). Immunofluorescence analysis of LC3B showed a decreased number of GFP-LC3B puncta in miR-200b-3p-overexpressing TFK-1 cells no matter with or without 5-FU treatment (Fig. 3A). Transmission electron microscopy revealed that number of autophagosomes/autolysosomes were significantly decreased in miR-200b-3p overexpressing TFK-1 cells regardless with or without 5-FU treatment (Fig. 3B). To confirm the effect of miR-200b-3p on autophagy, we evaluated LC3B II and p62 levels in the absence and presence of chloroquine (CQ), which inhibits autophagosome and lysosome fusion and LC3B II turnover. We observed that miR-200b-3p decreased LC3B II net turnover flux in TFK-1 and HuCCT-1 cells (Fig. 3C). Further, we measured autophagic flux using a tandem-labeled GFP-mRFP-LC3 reporter. This reporter localizes as yellow puncta in autophagosomes and red-only puncta in

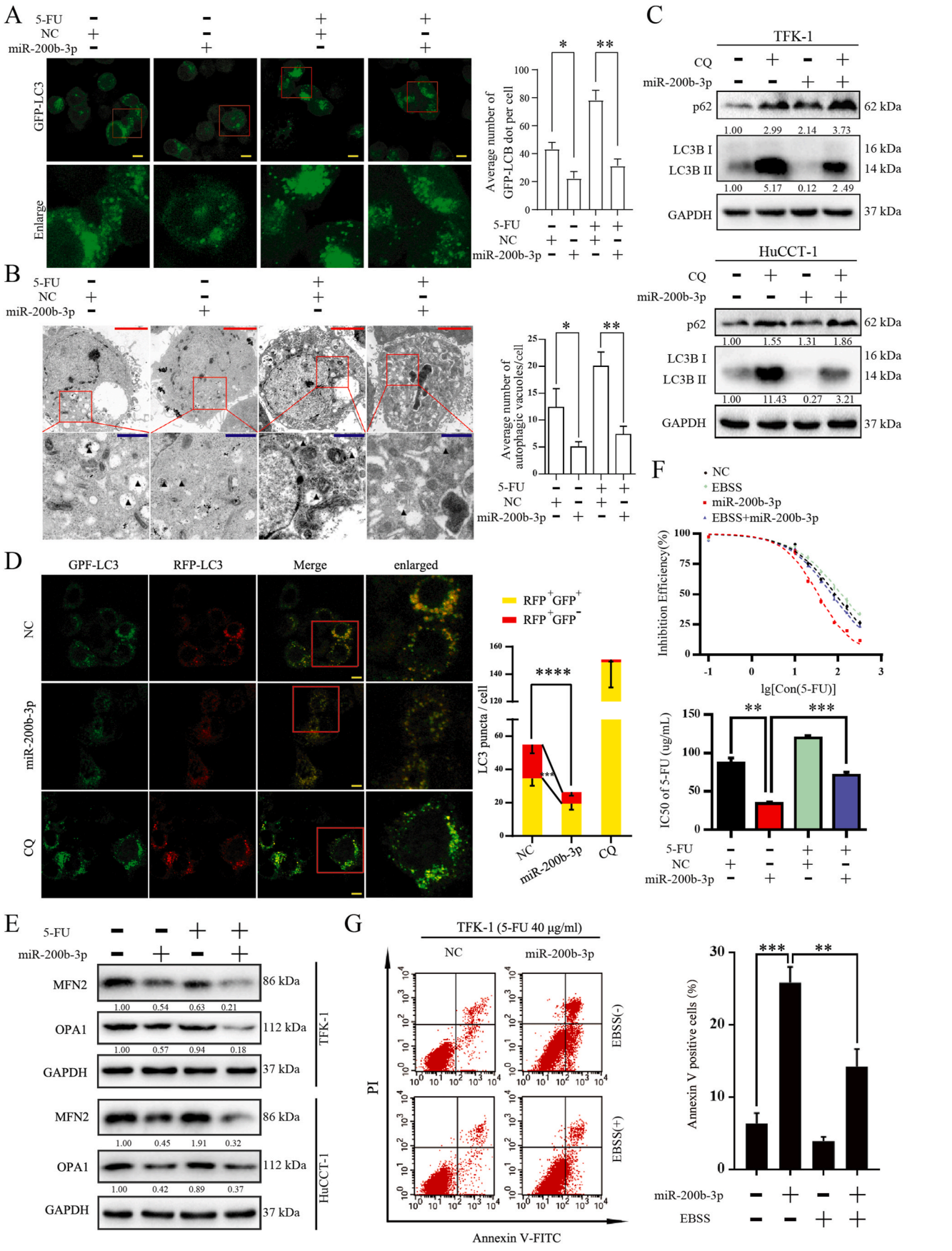

(caption on next page)

Fig. 3. MiR-200b-3p mediates 5-FU sensitivity by suppressing autophagy in CCA cells. (A) Immunofluorescence analysis showing LC3 puncta in TFK-1 cells stably expressing NC or miR-200b-3p in the absence or presence of 40 μg/mL of 5-FU treatment. Representative confocal images are shown in the left panel; the number of LC3 dots is quantified in the right panel. *p < 0.05; **p < 0.01; Scale bar: 10 μm. (B) Transmission electron microscopy showing autophagosomes/autolysosomes in TFK-1 cells stably expressing NC or miR-200b-3p in the absence or presence of 40 μg/mL of 5-FU treatment. Representative images and their magnified views are presented in the left panel. The right panel presents the quantification of the number of autophagic vacuoles. Triangle: autophagic vacuoles; *p < 0.05; **p < 0.01; Scale bar: 10 μm. (C) Western blot analysis of LC3B and p62 expression in TFK-1 and HuCCT-1 cells stably expressing NC or miR-200b-3p in the absence or presence of CQ treatment (10 μM, 24 h). (D) TFK-1 cells pre-transfected with GFP-mRFP-LC3B were transfected with NC or miR-200b-3p in the absence or presence of CQ treatment (10 μM, 24 h). Representative confocal images of autophagosome (yellow puncta) and autolysosome (red puncta) formation are presented in the left panel. Scale bar: 10 μm. The numbers of $RFP^{+}GFP^{+}$ LC3 puncta and $RFP^{+}GFP^{-}$ LC3 puncta are shown in the right panel. ****p < 0.0001 compared with the control. (E) Western blot analysis of MFN2 and OPA1 expression in TFK-1 and HuCCT-1 cells stably expressing NC or miR-200b-3p in the absence or presence of 40 μg/mL of 5-FU treatment. (F) TFK-1 cells stably expressing NC or miR-200b-3p in the absence or presence of EBSS treatment (24 h) were evaluated for cell sensitivity to 5-FU using the CCK8 assay upon exposure to step-up concentrations of 5-FU for 24 h. Dose-effect curves and statistical analysis of IC50 values are presented in the upper and lower panels, respectively. **p < 0.01; ***p < 0.001. (G) Flow cytometry detecting apoptotic cells in TFK-1 cells stably expressing NC or miR-200b-3p in the absence or presence of EBSS treatment (24 h) in the absence or presence of 40 μg/mL of 5-FU. **p < 0.01; ***p < 0.001.

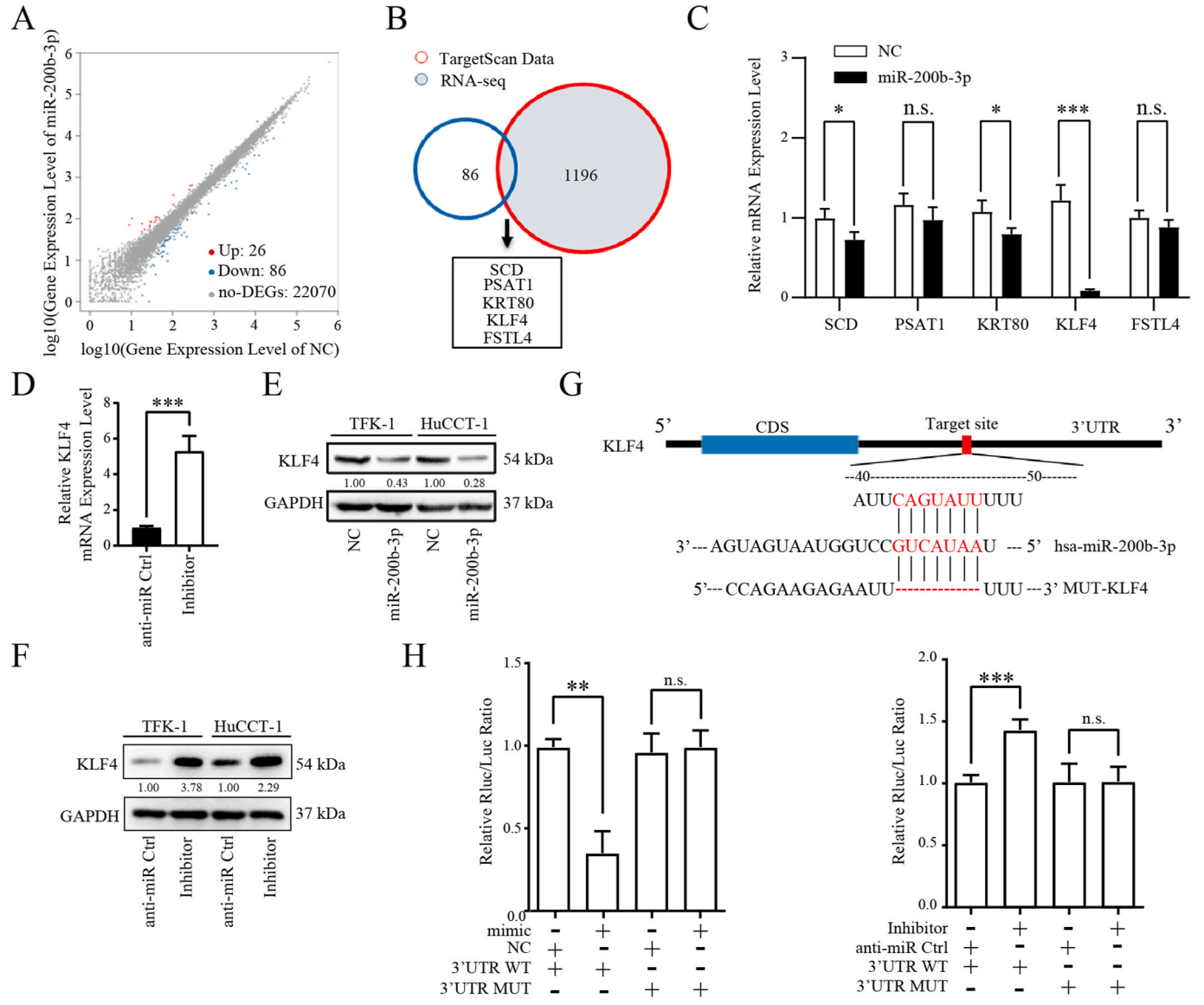

Fig. 4. *KLF4* is a key target gene of miR-200b-3p in CCA. (A) Differentially expressed genes with over 2-fold change in expression in TFK-1 cells transfected with miR-200b-3p compared with NC. (B) Schematic illustration of target genes of miR-200b-3p analysis based on TargetScan and RNA-seq data. (C) Real-time PCR analysis of five candidate genes in TFK-1 cells expressing NC or miR-200b-3p. (D) Real-time PCR analysis of KLF4 in TFK-1 cells transfected with miR-200b-3p inhibitor and its control. (E) Western blot analysis of KLF4 in TFK-1 or HuCCT-1 cells expressing NC or miR-200b-3p. (F) Western blot analysis of KLF4 in TFK-1 or HuCCT-1 cells transfected with miR-200b-3p inhibitor and its control. (G) Sequence alignment of miR-200b-3p with human wild-type (WT) and mutant 3′-UTR of *KLF4* mRNA. Binding site and seed region of miR-200b-3p are indicated in red. (H) Effects of miR-200b-3p mimic and miR-200b-3p inhibitor on the activity of WT or mutant KLF4 3′UTR luciferase reporter plasmid measured using a luciferase assay in TFK-1 cells.

autolysosomes, as the GFP fluorescence decays in the acidic lysosomal environment, whereas mRFP is more resistant to low pH [21]. Elevated miR-200b-3p decreased the number of total LC3 puncta compared to that in the control group, especially the number of red-only LC3 puncta in TFK-1 cells, indicating an inhibition of autophagic flux (Fig. 3D). In order to ascertain the impact of miR-200b-3p at the autophagosome level, we examined LAMP1 expression in CCA cells that overexpress miR-200b-3p. Immunofluorescence and western blot analysis revealed that overexpressed miR-200b-3p had no effect on the expression of the LAMP1 (Figs. S1A and B). Moreover, miR-200b-3p decreased the expression of mitochondrial fusion proteins (MFN2 and OPA1), and miR-200b-3p overexpression augmented the decrease in levels of these proteins in the presence of 5-FU (Fig. 3E). These results demonstrate that miR-200b-3p suppresses mitophagy in CCA cells.

Given that treatment with Earle's balanced salt solution (EBSS) induces autophagic flux in cells [22], we used EBSS as a positive control for autophagy inducers. And it has also been confirmed that EBSS has an impact on autophagic flux by western blot analysis (Fig. S1C). To verify the role of autophagy inhibition in miR-200b-3p-induced enhancement of 5-FU sensitivity, we treated miR-200b-3p-overexpressing and control CCA cells with EBSS using CCK8 assays to obtain IC50 values of 5-FU. We observed that EBSS treatment increased the IC50 values of 5-FU in miR-200b-3p-overexpressing CCA cells, that is, miR-200b-3p-induced 5-FU sensitivity was abolished by EBSS (Fig. 3F). Flow cytometric analysis of apoptosis revealed that EBSS treatment significantly weakened the miR-200b-3p-elicited apoptotic effect in the presence of 5-FU (Fig. 3G). These results suggest that inhibition of autophagy mediates miR-200b-3p-induced 5-FU sensitivity. Collectively, these data indicate that miR-200b-3p suppresses autophagy in CCA cells to mediate 5-FU sensitivity.

3.4. KLF4 is a key target gene of miR-200b-3p in CCA

To elucidate the direct downstream genes involved in miR-200b-3p-mediated effects on 5-FU sensitivity, RNA sequencing was performed to analyze the global gene expression profiles of miR-200b-3p-overexpressing and relevant control TFK-1 cells. Comparative gene expression of miR-200b-3p-overexpressing and control cells revealed changes in the expression of 112 genes (defined as >2- or <0.5- fold change with qValue ≤0.001), of which 86 were downregulated (Fig. 4A). GO analysis indicated that the downstream genes were mainly involved in cellular metabolic related functions. And the KEGG pathway analysis indicated that the downstream genes were associated with metabolic related pathways (Figs. S1A and B). In total, 1196 potential target genes of miR-200b-3p were predicted using the online bioinformatics program TargetScan 7.2 in *Homo sapiens* [23]. We compared the data derived from TargetScan7.2 (predicted targets of miR-200b-3p) and RNA-seq. Five genes were preliminarily identified as potential targets of miR-200b-3p in CCA, including *SCD, PSAT1, KRT80, KLF4*, and *FSTL4* (Fig. 4B). To further assess potential miR-200b-3p target genes, we validated the expression of these genes in miR-200b-3p-overexpressing cells using real-time PCR and western blotting. Among these genes, *KLF4* mRNA and protein levels were decreased with miR-200b-3p overexpression (Fig. 4C and E). Meanwhile, *KLF4* mRNA and protein levels were increased upon miR-200b-3p inhibition (Fig. 4D and F). Evaluation of the 3′-UTR sequences of *KLF4* in *Homo sapiens* revealed that *KLF4* contains a classical and conserved miR-200b-3p complementary site (Fig. 4G). Furthermore, luciferase reporter assays indicated that the luciferase activity of the reporter containing wild-type KLF4 3′-UTR was significantly reduced and increased by miR-200b-3p overexpression and knockdown, respectively. In contrast, overexpression or knockdown of miR-200b-3p did not alter the luciferase activity of the reporter containing the mutated KLF4 3′-UTR sequence (Fig. 4H). Collectively, these data suggest that *KLF4* is a direct target of miR-200b-3p in CCA cells.

3.5. MiR-200b-3p targets KLF4 mediated autophagy inhibition to enhance 5-FU sensitivity in CCA cells

KLF4 has been implicated in the regulation of mitochondrial homeostasis in cancer cells [24]. Mitochondria are highly dynamic and can undergo fusion, fission, and autophagy with changes in the tumor microenvironment [24,25]. To examine the involvement of KLF4 in miR-200b-3p-induced autophagy in CCA cells, western blotting was performed to analyze LC3B II and p62 levels in CCA cells. KLF4 overexpression enhanced LC3B II expression and attenuated miR-200b-3p-elicited reduction in LC3B II levels (Fig. 5A). It also decreased p62 and altered miR-200b-3p-elicited accumulation in p62 levels (Fig. 5A). Autophagic flux of miR-200b-3p and KLF4 were analyzed using tandem-labeled GFP-mRFP-LC3 reporter assays. KLF4 upregulation increased the number of GFP-mRFP-LC3-labeled yellow puncta and red-only LC3 puncta significantly and reversed miR-200b-3p-elicited changes in the number of LC3 puncta in TFK-1 cells (Fig. 5B). These data suggest that miR-200b-3p suppresses autophagy in CCA cells by downregulating KLF4 expression. To understand the role of KLF4 in autophagy mediated 5-FU sensitivity, we knocked down KLF4 in TFK-1 cells with or without EBSS treatment. Downregulated KLF4 reduced the IC50 values of 5-FU and EBSS treatment abrogated the decrease of it under knockdown of KLF4 (Fig. 5C). Flow cytometric analysis of apoptosis revealed KLF4 knockdown enhanced the apoptotic ratio of TFK-1 cells. And EBSS significantly counteracted the KLF4 depletion-dependent apoptotic effect of CCA cells (Fig. 5D). These results suggest that miR-200b-3p targets KLF4 mediated autophagy inhibition to enhance 5-FU sensitivity in CCA cells.

3.6. MiR-200b-3p/KLF4 pathway augments the chemosensitivity of CCA cells to 5-FU

To determine whether miR-200b-3p mediates 5-FU sensitivity by modulating KLF4, we overexpressed KLF4 in CCA cells by upregulating miR-200b-3p to assess the IC50 values of 5-FU. KLF4 overexpression increased the IC50 values of 5-FU in both miR-200b-3p-overexpressing and control CCA cells and reversed the decrease in IC50 values elicited by miR-200b-3p. These results indicated that miR-200b-3p-induced 5-FU sensitivity was abolished by KLF4 (Fig. 6A). Colony formation assays revealed that KLF4 also significantly rescued the reduction in clone number caused by miR-200b-3p in TFK-1 cells treated with 5-FU particularly (Fig. 6B). Consistent with these findings, KLF4 counteracted the decrease in PARP expression and partially offset the induction of PARP cleavage in both the absence and presence of 5-FU (Fig. 6C). Similar effects were confirmed using an annexin V-FITC/PI apoptosis assay (Fig. 6D).

To translate the results reported above *in vivo*, we established CCA xenograft models with subcutaneously implanted TFK-1 cells expressing control or miR-200b-3p with or without KLF4 overexpression. Tumor-bearing mice were intraperitoneally administered either vehicle or 5-FU twice per week. In the seventh week, KLF4 overexpression abrogated the miR-200b-3p induced suppression of tumor size in the absence or presence of 5-FU (Fig. 6E and F). Immunohistochemistry staining revealed that KLF4 resulted in a significant increase of Ki67 positive cells in miR-200b-3p overexpression treatment in the absence or presence of 5-FU (Fig. 6G and H). These findings highlight KLF4 as a major effector that participates in miR-200b-3p-regulated 5-FU sensitivity of CCA cells. These data provide evidence that the miR-200b-3p/KLF4 pathway plays a key role in promoting the chemosensitivity of CCA cells to 5-FU.

3.7. Aberrant expression of KLF4 in CCA

To assess the clinical relevance of KLF4 in CCA, we examined KLF4 expression in paired CCA and adjacent normal tissue samples. Western blot analysis of 12 cases revealed that KLF4 levels were higher in most of CCA samples than in normal tissue samples (Fig. 7A). Real-time PCR of

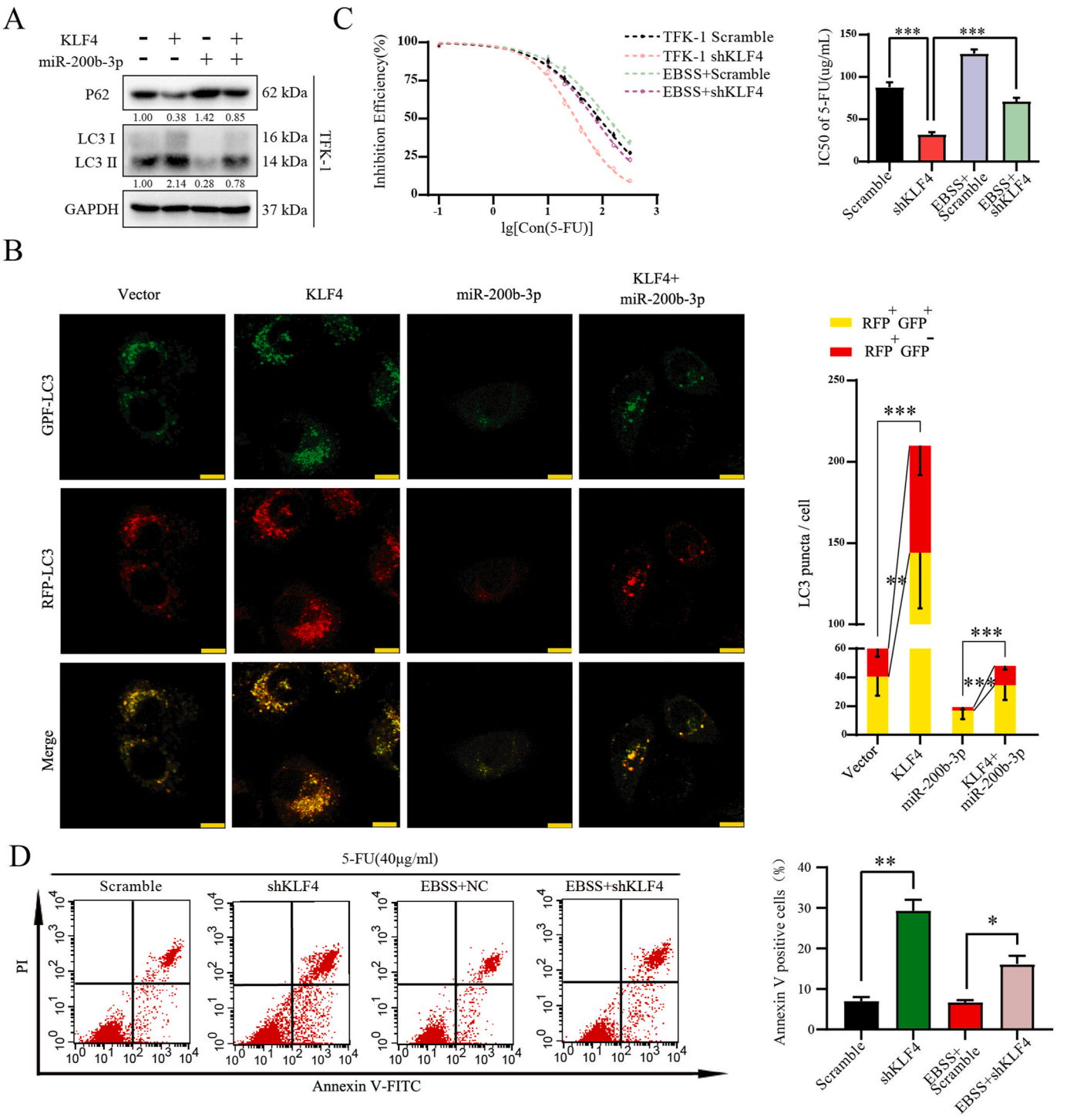

Fig. 5. miR-200b-3p targets KLF4 mediated autophagy inhibition to enhance 5-FU sensitivity in CCA cells. (A) Western blot analysis of LC3B and p62 expression in TFK-1 cells expressing NC or miR-200b-3p with or without KLF4 overexpression. (B) TFK-1 cells pre-transfected with GFP-mRFP-LC3B were transfected with NC or miR-200b-3p with or without KLF4 overexpression. Representative confocal images of autophagosome (yellow puncta) and autolysosome (red puncta) formation are presented in the left panel. Scale bar: 10 μm. The numbers of RFP^+GFP^+ LC3 puncta and RFP^+GFP^- LC3 puncta are presented in the right panel. $^{**}p < 0.01$; $^{***}p < 0.001$. (C) TFK-1 cells stably expressing NC or shKLF4 in the absence or presence of EBSS treatment (24 h) were evaluated for cell sensitivity to 5-FU using the CCK8 assay upon exposure to step-up concentrations of 5-FU for 24 h. Dose-effect curves and statistical analysis of IC50 values are presented in the left and right panels, respectively. $^{***}p < 0.001$. (D) Flow cytometry detecting apoptotic cells in TFK-1 cells stably expressing NC or shKLF4 in the absence or presence of EBSS treatment (24 h) in the absence or presence of 40 μg/mL of 5-FU.

30 cases indicated that KLF4 levels were higher in approximately 67% of CCA cancer tissues than in pair-matched adjacent normal tissues (Fig. 7B). Immunohistochemistry assays revealed that KLF4 expression levels were significantly higher in CCA tissues than in adjacent normal tissue samples (Fig. 7C and D). Collectively, these data indicate that the KLF4 expression is elevated in CCA.

4. Discussion

CCA is the second most common primary hepatic malignancy, with

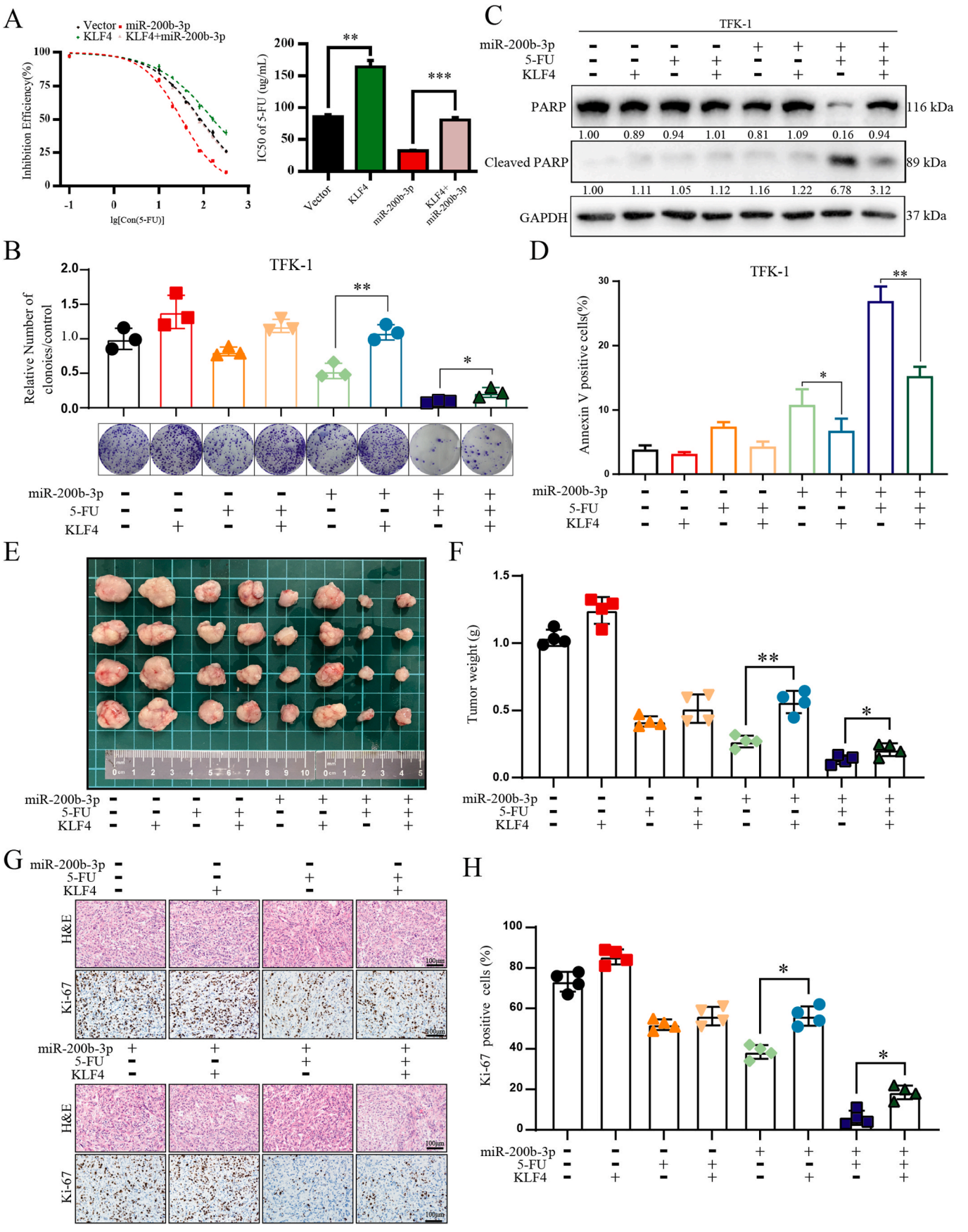

(caption on next page)

Fig. 6. miR-200b-3p/KLF4 pathway augments the chemosensitivity of CCA cells to 5-FU. (A) TFK-1 cells stably expressing NC or miR-200b-3p with or without KLF4 overexpression were evaluated for cell sensitivity to 5-FU using the CCK8 assay upon exposure to step-up concentrations of 5-FU for 24 h. Dose-effect curves and statistical analysis of IC50 values are presented in the upper and lower panels, respectively. **p < 0.01; ***p < 0.001. (B) Representative images of the colony-forming assay and colony number analysis of TFK-1 cells stably expressing NC or miR-200b-3p with or without KLF4 overexpression in the absence or presence of 40 μg/mL of 5-FU treatment, as indicated. All experiments were performed in triplicate. Data are presented as the mean ± SD. (C) Western blot analysis of PARP and cleaved PARP in TFK-1 cells stably expressing NC or miR-200b-3p with or without KLF4 overexpression in the absence or presence of 5-FU treatment, as indicated. (D) Flow cytometry detecting apoptotic cells in TFK-1 cells stably expressing NC or miR-200b-3p with or without KLF4 overexpression in the absence or presence of 5-FU treatment, as indicated. *p < 0.05; **p < 0.01. (E) Xenograft tumors from mice in each group in week 7 after implantation were excised and photographed are presented. (F) Weight analysis of subcutaneous tumors from the indicated groups. (G) Representative images of immunohistochemistry staining showing H&E and Ki67 in xenograft tumor tissues from the indicated groups. Scale bar, 100 μm. (H) Statistical analysis of percentage of Ki67 positive cells from xenograft tumor tissues as indicated.

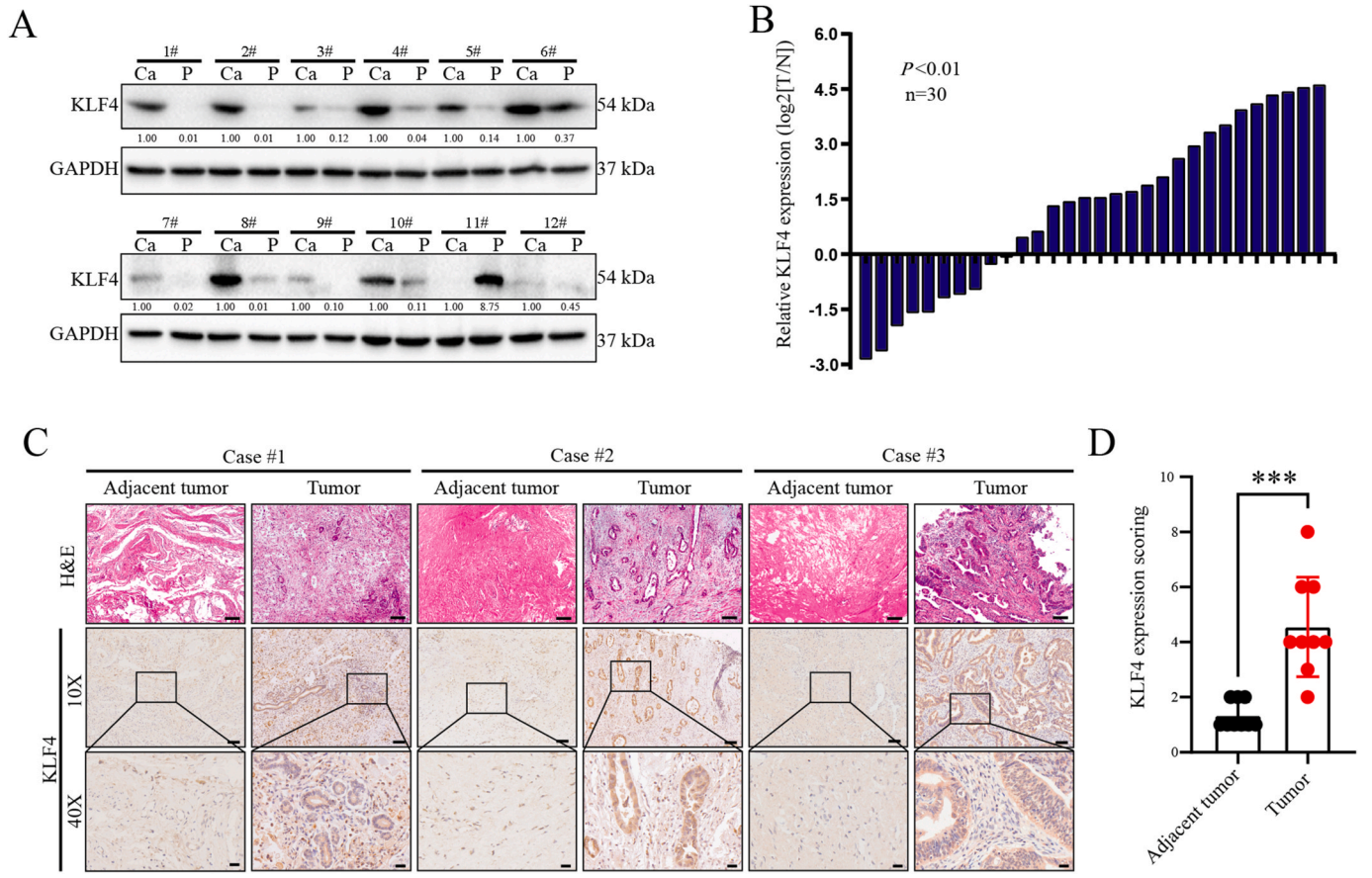

Fig. 7. Aberrant expression of KLF4 in CCA. (A) Western blot analysis of KLF4 protein expression in 12 samples of paired CCA tissues. (B) Real-time PCR showing relative mRNA levels of KLF4 in 30 samples of paired CCA tissues. (C-D) Immunohistochemical analysis of KLF4 in serial sections of 9 paired CCA tissues. Representative images are shown in the (C). Statistical analysis of KLF4 expression is in the (D). Scale bar in image at 10 × magnification: 100 μm; scale bar in image at 40 × magnification: 20 μm.

an increasing incidence and mortality worldwide [26]. Due to the absence of specific symptoms, early diagnosis of CCA is challenging. As a result, patients may present at an advanced stage only to undergo chemotherapy rather than surgery [27,28]. Chemoresistance is a complex phenomenon that underscores failure to respond to chemotherapy agents and contributes to more than 90% of deaths in patients with cancer [29]. 5-FU is a widely used chemotherapy for multiple types of gastrointestinal cancers, including CCA. Therefore, understanding the mechanisms of chemoresistance in CCA is critical to improve patient survival. miRNAs are regulatory non-coding RNAs that play key roles in disease recurrence and progression [30]. Accordingly, identifying candidate miRNAs that regulate CCA chemotherapy resistance may facilitate the development of effective treatments. We previously established a profile of dysregulated miRNAs in CCA tissues and identified miR-200 family members as one of the top six downregulated miRNAs that inhibit CCA tumorigenesis and metastasis [16]. Further, the exosomal miR-200 family has been identified as a serum biomarker for the early detection and prognostic prediction of CCA [31]. In this study, we demonstrated that miR-200b-3p enhances the chemosensitivity of CCA cells to 5-FU, and miR-200b-3p-induced mitochondrial apoptosis plays a key role in the regulation of chemosensitivity to 5-FU. These findings highlight miR-200b-3p as a potential marker of sensitivity to chemotherapeutic drugs for CCA.

Autophagy is a conserved homeostatic process in CCA cells that promotes cell survival following targeted therapy [6]. The effects of autophagy on cancer are complex [32], but this process supports cancer growth in extreme environments, including exposure to chemotherapeutics [33]. Substantial evidence indicates that crosstalk between autophagic and apoptotic pathways is induced during chemotherapeutic cellular damage [34]. Autophagy induces resistance in a wide range of cancer cells. Indeed, inhibition of autophagy has been reported to overcome chemoresistance in many tumor cells [35]. In our model, we

observed that miR-200b-3p suppressed autophagy in CCA cells. Further, miR-200b-3p-elicited 5-FU sensitivity was abolished by EBSS-induced autophagic flux in CCA cells, indicating that miR-200b-3p suppresses autophagy to mediate 5-FU sensitivity. These findings are in accordance with our previous data demonstrating that miR-200b/c inhibits the invasion and metastatic properties of CCA cells [16].

It is well established that miRNAs regulate downstream target genes via assembly of RISC at the transcriptional and post-transcriptional levels [13], indicating that miRNAs may target multiple mRNAs. To elucidate the underlying mechanisms by which miR-200b-3p enhances the chemosensitivity of CCA cells to 5-FU, we screened for potential targets for chemotherapeutic sensitization. RNA-seq and the computational prediction program TargetScan7.2 were used for the primary screening, and RT-PCR and western blotting were used for verification. In our study, *KLF4*, one of the five candidate targets screened with TargetScan7.2 (predicted targets of miR-200b-3p), overlapped with the 86 downregulated genes that were differentially expressed and was identified to be regulated by miR-200b-3p in CCA. Indeed, we verified that miR-200b-3p significantly inhibited KLF4 expression at both the transcriptional and post-transcriptional levels in CCA cells. Luciferase assays confirmed that KLF4 was a direct target of miR-200b-3p in CCA cells. Altogether, these results suggest that KLF4 is an essential target for miR-200b-3p to perform its potential biological functions.

KLF4 is a crucial self-renewal transcriptional factor of the KLF family that exerts diverse modulatory effects in proliferation, differentiation, and somatic cell reprogramming [36]. KLF4 is involved in the induction of pluripotent stem cells and mediates autophagy flux to regulate metabolic homeostasis, including mitochondrial homeostasis, in response to stress [24,37]. KLF4-associated autophagy (mitophagy) plays a key role in apoptosis associated with mitochondrial dysfunctional and reactive oxygen species (ROS)-mediated cellular damage [25,38]. We thus hypothesized that KLF4 was involved in autophagy-mediated miR-200b-3p-induced mitochondrial apoptosis in CCA cells and increased chemosensitivity to 5-FU. In the present study, we demonstrated that KLF4 downregulation was involved in miR-200b-3p-mediated suppression of autophagy in CCA cells, implicating KLF4 as a major effector in miR-200b-3p-regulated 5-FU sensitivity in CCA cells. Further, we observed that the expression of KLF4 was elevated in CCA. These data provide evidence that miR-200b-3p targets KLF4 and suppresses autophagy, thereby elevating 5-FU sensitivity in CCA cells.

In summary, this study demonstrates that miR-200b-3p enhances the chemosensitivity of CCA cells to 5-FU. Our results indicate that autophagy modulates 5-FU chemoresistance in CCA cells via the miR-200b-3p/KLF4 axis. The current findings suggest that the miR-200b-3p/KLF4/autophagy pathway plays a pivotal role in promoting the chemosensitivity of CCA cells to 5-FU. These findings highlight the potential utility of targeting the miR-200b-3p/KLF4/autophagy axis for increase the efficacy of chemotherapeutics for CCA.

Funding

This study was supported by the National Natural Science Foundation of China (No. 82103452 to Ruizhi He, No. 81402443 to Feng Peng, No. 81772950 to Renyi Qin).

Data availability

The datasets used and analyzed during the current study are available from the corresponding author on reasonable request.

Competing interests

The authors have no conflicts of interest to declare.

Ethics approval and consent to participate

Our studies were approved by the Ethics Committee of the Tongji Hospital, Tongji Medical College, Huazhong University of Science and Technology (TJH-202006008).

Consent for publication

We have obtained consents to publish this paper from all the participants of this study.

CRediT authorship contribution statement

Feng Peng: Writing – review & editing, Supervision, Conceptualization. **Ruizhi He:** Writing – original draft, Funding acquisition, Data curation. **Yuhui Liu:** Investigation, Formal analysis. **Yu Xie:** Software, Resources. **Guangbing Xiong:** Visualization, Software. **Xu Li:** Methodology, Investigation. **Min Wang:** Validation, Formal analysis. **Chunle Zhao:** Writing – original draft, Investigation, Formal analysis. **Hang Zhang:** Writing – original draft, Supervision, Data curation. **Simiao Xu:** Visualization, Supervision, Methodology. **Renyi Qin:** Writing – review & editing, Supervision, Funding acquisition, Conceptualization.

Declaration of competing interest

The authors declare that they have no known competing financial interests or personal relationships that could have appeared to influence the work reported in this paper.

Acknowledgements

Not applicable.

Abbreviations

CCA	cholangiocarcinoma
5-FU	5-fluorouracil
miRNA	microRNA
RISC	RNA-induced silencing complex
3′-UTR	3′-untranslated region
KLF4	Krüppel-like factor 4
CCK-8	cell counting kit-8
Δψm	mitochondrial membrane potential
CQ	chloroquine; EBSS: Earle's balanced salt solution

Appendix A. Supplementary data

Supplementary data to this article can be found online at https://doi.org/10.1016/j.ncrna.2024.06.004.

References

[1] R. Kelley, N. Bardeesy, Biliary Tract cancers: finding better ways to lump and split, J. Clin. Oncol. 33 (2015) 2588–2590, https://doi.org/10.1200/jco.2015.61.6953.
[2] E. Ben-Josef, K.A. Guthrie, A.B. El-Khoueiry, C.L. Corless, M.M. Zalupski, A. M. Lowy, et al., Swog S0809: a phase II intergroup trial of adjuvant capecitabine and gemcitabine followed by radiotherapy and concurrent capecitabine in extrahepatic cholangiocarcinoma and gallbladder carcinoma, J. Clin. Oncol. 33 (2015) 2617–2622, https://doi.org/10.1200/jco.2014.60.2219.
[3] Z.F. Hong, W.X. Zhao, Z.Y. Yin, C.R. Xie, Y.P. Xu, X.Q. Chi, et al., Capsaicin enhances the drug sensitivity of cholangiocarcinoma through the inhibition of chemotherapeutic-induced autophagy, PLoS One 10 (2015) e0121538, https://doi.org/10.1371/journal.pone.0121538.
[4] A.E. Sirica, Cholangiocarcinoma: molecular targeting strategies for chemoprevention and therapy, Hepatology 41 (2005) 5–15, https://doi.org/10.1002/hep.20537. Baltimore, Md.
[5] S. Thongprasert, The role of chemotherapy in cholangiocarcinoma, Ann. Oncol. : official journal of the European Society for Medical Oncology 16 (Suppl 2) (2005) ii93–96, https://doi.org/10.1093/annonc/mdi712.

[6] L. Yu, Y. Chen, S.A. Tooze, Autophagy pathway: cellular and molecular mechanisms, Autophagy 14 (2018) 207–215, https://doi.org/10.1080/15548627.2017.1378838.
[7] Y.G. Zhao, P. Codogno, H. Zhang, Machinery, regulation and pathophysiological implications of autophagosome maturation, Nat. Rev. Mol. Cell Biol. 22 (2021) 733–750, https://doi.org/10.1038/s41580-021-00392-4.
[8] L.E. Drake, M.Z. Springer, L.P. Poole, C.J. Kim, K.F. Macleod, Expanding perspectives on the significance of mitophagy in cancer, Semin. Cancer Biol. 47 (2017) 110–124, https://doi.org/10.1016/j.semcancer.2017.04.008.
[9] A.C. Kimmelman, E. White, Autophagy and tumor metabolism, Cell Metabol. 25 (2017) 1037–1043, https://doi.org/10.1016/j.cmet.2017.04.004.
[10] E. White, The role for autophagy in cancer, The Journal of clinical investigation 125 (2015) 42–46, https://doi.org/10.1172/jci73941.
[11] H. Perez-Montoyo, Therapeutic potential of autophagy modulation in cholangiocarcinoma, Cells 9 (2020), https://doi.org/10.3390/cells9030614.
[12] D.P. Bartel, MicroRNAs: genomics, biogenesis, mechanism, and function, Cell 116 (2004) 281–297, https://doi.org/10.1016/s0092-8674(04)00045-5.
[13] R.W. Carthew, E.J. Sontheimer, Origins and Mechanisms of miRNAs and siRNAs, Cell 136 (2009) 642–655, https://doi.org/10.1016/j.cell.2009.01.035.
[14] R. Rupaimoole, F.J. Slack, MicroRNA therapeutics: towards a new era for the management of cancer and other diseases, Nat. Rev. Drug Discov. 16 (2017) 203–222, https://doi.org/10.1038/nrd.2016.246.
[15] F. Meng, R. Henson, M. Lang, H. Wehbe, S. Maheshwari, J.T. Mendell, et al., Involvement of human micro-RNA in growth and response to chemotherapy in human cholangiocarcinoma cell lines, Gastroenterology 130 (2006) 2113–2129, https://doi.org/10.1053/j.gastro.2006.02.057.
[16] F. Peng, J. Jiang, Y. Yu, R. Tian, X. Guo, X. Li, et al., Direct targeting of SUZ12/ROCK2 by miR-200b/c inhibits cholangiocarcinoma tumourigenesis and metastasis, British journal of cancer 109 (2013) 3092–3104, https://doi.org/10.1038/bjc.2013.655.
[17] M.A. Indap, S.G. Rao, Cell death by apoptosis and cancer chemotherapy, The National medical journal of India 8 (1995) 65–67.
[18] N.J. Curtin, C. Szabo, Poly(ADP-ribose) polymerase inhibition: past, present and future, Nat. Rev. Drug Discov. 19 (2020) 711–736, https://doi.org/10.1038/s41573-020-0076-6.
[19] F. Guerra, A.A. Arbini, L. Moro, Mitochondria and cancer chemoresistance, Biochimica et biophysica acta. Bioenergetics 1858 (2017) 686–699, https://doi.org/10.1016/j.bbabio.2017.01.012.
[20] M. Vara-Perez, B. Felipe-Abrio, P. Agostinis, Mitophagy in cancer: a tale of adaptation, Cells (2019) 8, https://doi.org/10.3390/cells8050493.
[21] R. He, M. Wang, C. Zhao, M. Shen, Y. Yu, L. He, et al., TFEB-driven autophagy potentiates TGF-β induced migration in pancreatic cancer cells, J. Exp. Clin. Cancer Res. : CR 38 (2019) 340, https://doi.org/10.1186/s13046-019-1343-4.
[22] D. Laha, M. Deb, H. Das, KLF2 (kruppel-like factor 2 [lung]) regulates osteoclastogenesis by modulating autophagy, Autophagy 15 (2019) 2063–2075, https://doi.org/10.1080/15548627.2019.1596491.
[23] TargetScan7.2 (miR-200b-3p predicted targets) dataset. TargetScan Human, USA. http://www.targetscan.org/vert_72/. Accessed 8 January 2019.
[24] A.M. Ghaleb, V.W. Yang, Krüppel-like factor 4 (KLF4): what we currently know, Gene 611 (2017) 27–37, https://doi.org/10.1016/j.gene.2017.02.025.
[25] W.M. Rosencrans, Z.H. Walsh, N. Houerbi, A. Blum, M. Belew, C. Liu, et al., Cells deficient for Krüppel-like factor 4 exhibit mitochondrial dysfunction and impaired mitophagy, European journal of cell biology 99 (2020) 151061, https://doi.org/10.1016/j.ejcb.2019.151061.
[26] K. Wang, H. Zhang, Y. Xia, J. Liu, F. Shen, Surgical options for intrahepatic cholangiocarcinoma, Hepatobiliary Surg. Nutr. 6 (2017) 79–90, https://doi.org/10.21037/hbsn.2017.01.06.
[27] S. Rizvi, S.A. Khan, C.L. Hallemeier, R.K. Kelley, G.J. Gores, Cholangiocarcinoma - evolving concepts and therapeutic strategies, Nat. Rev. Clin. Oncol. 15 (2018) 95–111, https://doi.org/10.1038/nrclinonc.2017.157.
[28] U. Cillo, C. Fondevila, M. Donadon, E. Gringeri, F. Mocchegiani, H.J. Schlitt, et al., Surgery for cholangiocarcinoma, Liver international, official journal of the International Association for the Study of the Liver 39 (Suppl 1) (2019) 143–155, https://doi.org/10.1111/liv.14089.
[29] Y. Jing, W. Liang, J. Liu, L. Zhang, J. Wei, J. Yang, et al., Autophagy-mediating microRNAs in cancer chemoresistance, Cell biology and toxicology 36 (2020) 517–536, https://doi.org/10.1007/s10565-020-09553-1.
[30] W. Huang, MicroRNAs: biomarkers, diagnostics, and therapeutics, Methods Mol. Biol. 1617 (2017) 57–67, https://doi.org/10.1007/978-1-4939-7046-9_4.
[31] L. Shen, G. Chen, Q. Xia, S. Shao, H. Fang, Exosomal miR-200 family as serum biomarkers for early detection and prognostic prediction of cholangiocarcinoma, Int. J. Clin. Exp. Pathol. 12 (2019) 3870–3876.
[32] E.E. Mowers, M.N. Sharifi, K.F. Macleod, Functions of autophagy in the tumor microenvironment and cancer metastasis, FEBS J. 285 (2018) 1751–1766, https://doi.org/10.1111/febs.14388.
[33] Y.J. Li, Y.H. Lei, N. Yao, C.R. Wang, N. Hu, W.C. Ye, et al., Autophagy and multidrug resistance in cancer, Chin. J. Cancer 36 (2017) 52, https://doi.org/10.1186/s40880-017-0219-2.
[34] S. Mukhopadhyay, P.K. Panda, N. Sinha, D.N. Das, S.K. Bhutia, Autophagy and apoptosis: where do they meet? Apoptosis : an international journal on programmed cell death 19 (2014) 555–566, https://doi.org/10.1007/s10495-014-0967-2.
[35] S. Piya, M. Andreeff, G. Borthakur, Targeting autophagy to overcome chemoresistance in acute myleogenous leukemia, Autophagy 13 (2017) 214–215, https://doi.org/10.1080/15548627.2016.1245263.
[36] D.C. Di Giammartino, A. Kloetgen, A. Polyzos, Y. Liu, D. Kim, D. Murphy, et al., KLF4 is involved in the organization and regulation of pluripotency-associated three-dimensional enhancer networks, Nat. Cell Biol. 21 (2019) 1179–1190, https://doi.org/10.1038/s41556-019-0390-6.
[37] A. Blum, K. Mostow, K. Jackett, E. Kelty, T. Dakpa, C. Ryan, et al., KLF4 regulates metabolic homeostasis in response to stress, Cells 10 (2021), https://doi.org/10.3390/cells10040830.
[38] C. Liu, E.P. DeRoo, C. Stecyk, M. Wolsey, M. Szuchnicki, E.G. Hagos, Impaired autophagy in mouse embryonic fibroblasts null for Krüppel-like Factor 4 promotes DNA damage and increases apoptosis upon serum starvation, Mol. Cancer 14 (2015) 101, https://doi.org/10.1186/s12943-015-0373-6.